

Structural damage detection by principle component analysis of long-gauge dynamic strains

Q. Xia, Y.D. Tian, X.W. Zhu, D.W. Xu and J. Zhang*

Key Laboratory of C&PC Structures of the Ministry of Education, Southeast University, Nanjing 210096, China

(Received December 16, 2014, Revised February 2, 2015, Accepted February 27, 2015)

Abstract. A number of acceleration-based damage detection methods have been developed but they have not been widely applied in engineering practices because the acceleration response is insensitive to minor damage of civil structures. In this article, a damage detection approach using the long-gauge strain sensing technology and the principle component analysis technology is proposed. The Long gauge FBG sensor has its special merit for damage detection by measuring the averaged strain over a long-gauge length, and it can be connected each other to make a distributed sensor network for monitoring the large-scale civil infrastructure. A new damage index is defined by performing the principle component analyses of the long-gauge strains measured from the intact and damaged structures respectively. Advantages of the long gauge sensing and the principle component analysis technologies guarantee the effectiveness for structural damage localization. Examples of a simple supported beam and a steel stringer bridge have been investigated to illustrate the successful applications of the proposed method for structural damage detection.

Keywords: principal component analysis; impact testing; long-gauge fiber optic sensor; Euclidean norm; damage detection

1. Introduction

Structural health monitoring (SHM) technology has been developed over fifty years, and it has been applied to a number of bridges and buildings (Montalvao *et al.* 2006, Zou *et al.* 2000, Lei *et al.* 2012). How to use the monitoring data to detect structural damages is important. A number of vibration-based damage detection techniques have been developed, including the damage indexes utilizing structural frequency shifts, mode shape changes, mode shape curvature changes, flexibility changes, or modal strain energy changes (Doebling *et al.* 1998, Bagchi *et al.* 2001, Catbas *et al.* 2006, Zhang *et al.* 2013, Aditi Majumdar *et al.* 2013, Rezaiee-Pajand *et al.* 2014, Arslan *et al.* 2014, Yazdanpanah *et al.* 2015).

Most damage detection approaches in the literature used structural modal parameters identified from acceleration measurements. Rucevskis and Wesolowski (2010) studied the applicability of the modal shape curvature squares determined from only the damaged state of a beam for damage detection. A flexibility-based two-stage procedure was presented by Kazemi *et al.* (2010) to localize structural faults and their corresponding severity in thin plate structures. An and Ou

*Corresponding author, Professor, E-mail: jian@seu.edu.cn

(2012) developed a curvature difference probability method for damage localization. Baseline-free methods have been developed for structural damage detection using the acceleration data only from the damaged structure (Yoon *et al.* 2005). Ratcliffe *et al.* (1997) developed the gapped smoothing method (GSM) operating solely on data obtained from the damaged structure to locate structural stiffness variability. Santos and Orcesi (2015) used the unsupervised discrimination machine-learning method for structural damage detection without the baseline structure. The above reviewed methods used acceleration responses for structural damage detection, however, it has been increasingly recognized that the acceleration is insensitive to structural minor damages (Conte *et al.* 2008, He *et al.* 2009).

In contrast, strain is considered as a good candidate for structural damage detection because it is sensitive to local damages. Alvandi and Cremona (2006) represented that the strain energy based methods is much more efficient than acceleration-based methods by considering the modal strain energy change before and after the damage occurs. Guan and Karbhari (2008) proposed an improved modal strain damage index without using numerical differentiation, which is considered to be the main cause for the poor performance of the modal curvature method. However, the strain has its limitation too for structural damage detection. Traditional strain gauges have very short gauge lengths, which makes it be difficult to find damages within huge and complex civil structures. Due to the limitation of traditional point-type strain gauges, a novel long-gauge fiber optic sensor has been developed. It has a long gauge length, for instance, 1~2 m, which means that it measures the averaged strain over the long gauge length. The long-gauge strain not only reflects local but also global information of the structure. Especially, the long-gauge sensors can be connected each other to make a distributed sensor network for monitoring the large-scale civil structures, they are much more suitable for structural damage detection (Li and Wu 2007, Wu and Zhang 2012).

Based on the advantage of the long gauge FBG sensor, a new damage index will be proposed by performing the principle component analysis of the long gauge dynamic strains under impact testing. In engineering practice, the monitoring data generally consists of much redundant information. The principal component analysis (PCA) is an effective technology to separate the influence of noise and environmental factors from “pure” data. Ni *et al.* (2006) identified the damage of a 38-floor building by performing the PCA to structural frequency response functions, and the results illustrated that it greatly improved the robustness of the damage detection method. Based on the merit of the PCA technology, a damage index will be proposed for effective structural damage detection with long gauge strain time histories.

In this article, the long-gauge FBG sensor and the framework of using the long-gauge strains and the PCA technology for damage detection will be introduced in section 2. Then, the details of the proposed method for structural damage detection will be presented in Section 3. Its procedure includes covariance matrix calculation, singular value decomposition, principle component confirmation, Euclidean norm calculation, and finally the damage index calculation. In sections 4 and 5, examples of a simply supported beam and a steel stringer bridge will be investigated to verify the effectiveness of the proposed method respectively. Finally, conclusions are drawn.

2. Framework of the proposed method

Structural dynamic responses (e.g., acceleration and strain) contain structural damage information. The relation between acceleration and damage characteristic is indirect, thus

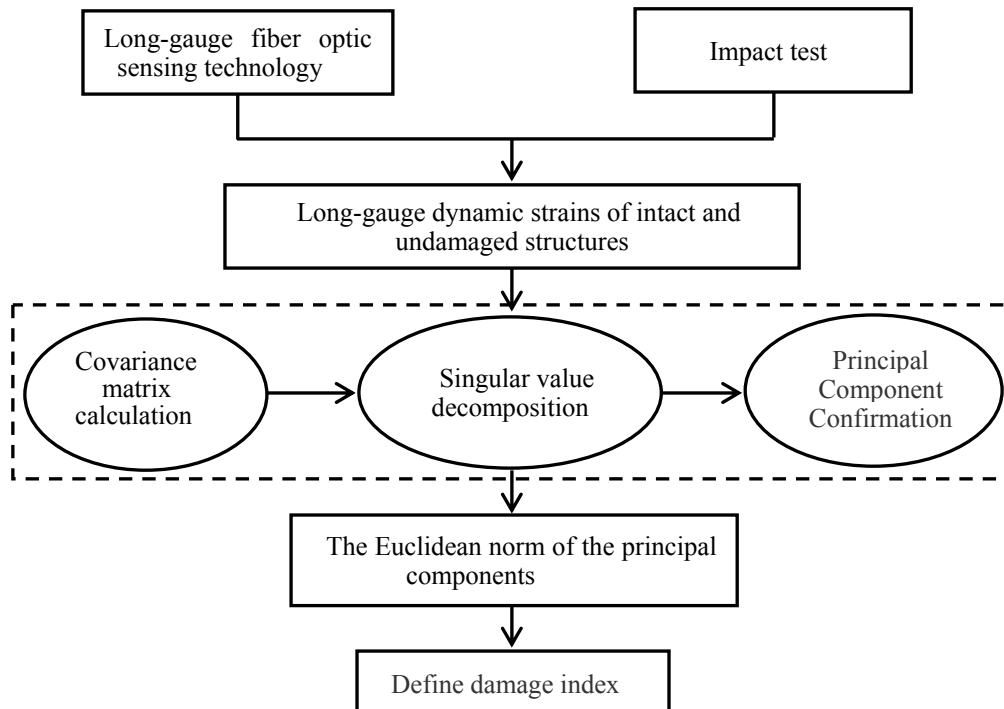


Fig. 1 Framework of the proposed method

acceleration-based damage indexes are insensitive to minor damages. Dynamic strains from traditional point-type strain gauges are sensitive to damages but they are too local to perform damage detection of large-scale civil structures. To overcome the limitations of acceleration- and point-type strain-based sensing technologies, the long-gauge FBG sensor as shown in Fig. 1 is developed by designing the FBG sensor with a long-gauge (e.g., 1-2 m) and fixing its two ends. Even though there are studies about the long-gauge sensor in the literature (Glišić and Inaudi 2007), the developed long-gauge FBG sensor has its unique feature. Technologies including the basalt fiber reinforcing, optical fiber anchoring and sensitivity enhancing have been developed to make the developed long gauge FBG sensor have high performance and long durability. The in-tube fiber has the same mechanical behavior of the structure, and hence the strain transferred from the shift of Bragg center wavelength represents the averaged strain over the long-gauge length. The developed sensor has the merit to measure the averaged strain over the long gauge length which is sensitive to the damages appeared within the gauge length. Moreover, the long-gauge sensors can be connected in series to make an FBG sensor array for distributed sensing. The above features offer the developed sensor the advantage of measuring both local and global information of the structure, thus it is potential to be applied for effective damage detection of large-scale civil structures.

A framework utilizing the long-gauge strain measurements and the PCA technology as shown in Fig. 1 is proposed for structural damage detection. Its procedure is described as follows:

Step 1: To perform impact testing on the intact and damaged structures respectively. Long-gauge FBG sensors are used to measure structural responses during the impact tests.

Step 2: To standardize the measured long-gauge strain data and calculate its principle

components. The theory of PCA and its detailed procedure will be described in next section.

Step 3: To calculate the averaged Euclidean norm of the principle components. Definition of the Euclidean norm will be given in next section.

Step 4: To obtain the proposed damage index by calculating the square of the averaged Euclidean norm change before and after damage occurring. The elements corresponding to high damage indexes denote damage locations.

Step 5: To calculate a damage index matrix by using a number of nodes as references to better show damage detection results. The matrix is a square one. If some rows and columns of that matrix have obvious changes, it indicates that damages occur on the corresponding elements.

3. Theory basis of the proposed method

3.1 Data normalization

Structural responses are determined by structural intrinsic characteristics and external forces. When structural responses are different with same external forces, it indicates that structural parameter changes, i.e., damages occur. Therefore, the task of damage detection is transformed to how to detect the change of structural responses when the external force is not changed. In order to eliminate the influence of observation noise, the measured long gauge strains are first normalized. Assuming m long gauge sensors are used to measure structural dynamic responses, and each measurement has a length of n , the following data matrix is generated by dividing each time series to p pieces

$$X_k = \begin{bmatrix} x_{k11} & x_{k12} & \cdots & x_{k1q} \\ x_{k21} & x_{k22} & \cdots & x_{k2q} \\ \vdots & \vdots & \ddots & \vdots \\ x_{km1} & x_{km2} & \cdots & x_{kmq} \end{bmatrix}_{m \times q} \quad (k = 1, 2, 3, \dots, p) \quad (1)$$

where q is the length of each piece of the data, i.e., $n = p \times q$. The data matrix as shown in Eq. (1) is normalized to Eq. (2)

$$X'_k = \begin{bmatrix} x'_{k11} & x'_{k12} & \cdots & x'_{k1q} \\ x'_{k21} & x'_{k22} & \cdots & x'_{k2q} \\ \vdots & \vdots & \ddots & \vdots \\ x'_{km1} & x'_{km2} & \cdots & x'_{kmq} \end{bmatrix}_{m \times q} \quad (k = 1, 2, 3, \dots, p) \quad (2)$$

where: $x'_{kij} = \frac{x_{kij} - x'_{kj}}{\sigma_{kj}}$, ($i = 1, 2, \dots, m; j = 1, 2, \dots, q$), x'_{kj} and σ_{kj} are the mean and variance of X_k .

3.2 Feature extraction by the PCA technology

First, the covariance matrix of the normalized data is calculated as follows

$$C_k = \frac{1}{m-1} X_{ki}'^T X_{ki}', (i = 1, 2, 3, \dots, m, k = 1, 2, 3, \dots, p) \quad (3)$$

where C_k is a square matrix with the dimension of $(q \times q)$.

Then, the singular value decomposition is performed to the covariance matrix

$$[U_k, S_k, V_k] = \text{svd}(C_k), (k = 1, 2, 3, \dots, p) \quad (4)$$

$$U_k = \begin{bmatrix} u_{k11} & \cdots & u_{k1q} \\ \vdots & \ddots & \vdots \\ u_{km1} & \cdots & u_{kmq} \end{bmatrix}_{m \times q}, V_k = \begin{bmatrix} v_{k11} & \cdots & v_{k1q} \\ \vdots & \ddots & \vdots \\ v_{km1} & \cdots & v_{kmq} \end{bmatrix}_{m \times q}, S_k = \begin{bmatrix} \lambda_{k1} & \cdots & 0 \\ \vdots & \ddots & \vdots \\ 0 & \cdots & \lambda_{kq} \end{bmatrix}_{q \times q} \quad (5)$$

$(k = 1, 2, 3, \dots, p)$

where U_k and V_k are left and right vector matrices, respectively, and S_k is the singular value matrix. By using the singular value matrix, the principal components are determined in the following way

$$\alpha_k = \frac{\sum_{j=1}^r \lambda_{kj}}{\sum_{j=1}^q \lambda_{kj}}, (k = 1, 2, 3, \dots, p) \quad (6)$$

$$PC_k = (X_k')_{m \times q} (U_k)_{q \times r} \quad (7)$$

$$PC_k = \begin{bmatrix} p_{k11} & \cdots & p_{k1r} \\ \vdots & \ddots & \vdots \\ p_{km1} & \cdots & p_{kmr} \end{bmatrix}_{m \times r} \quad (8)$$

where, α_k denotes the ratio of the sum of the first r components to the sum of all components. PC_k denotes the vector including the first r components, r is the principal component number, PC_k is the principal component matrix. The value of α_k is selected based on the tradeoff between the accuracy and the computation time. When α_k equals 1, all singular values will be used in Eq. (6), which will produce the most accurate result but taking the most computation time. It is selected to be 0.9 in this article.

3.3 Damage index definition

Euclidean norm of the principal component is calculated by summing the squares of all pieces of the data and taking the square root

$$E_{\text{norm}} = \begin{bmatrix} e_{11} & \cdots & e_{1p} \\ \vdots & \ddots & \vdots \\ e_{m1} & \cdots & e_{mp} \end{bmatrix}_{m \times p} \quad (9)$$

$$e_{ik} = \sqrt{(p_{ki1}^2 + p_{ki2}^2 + \dots + p_{kir}^2)}, (i=1,2,\dots,m; k=1,2,3,\dots,p) \quad (10)$$

where p_{kir} is a principle component element as shown in Eq. (8).

By performing the impact tests of the intact and damaged structures respectively, structural strain responses are measured by using the long-gauge FBG sensors. Their principle component matrices and Euclidean norms are calculated by using Eq. (10) and Eq. (9) respectively. Thereafter, a new damage index is defined by using the Euclidean norm of the principle components as follows

$$DI = \left(\frac{E^d - E^u}{E^u} \right)^2 \quad (11)$$

$$E^u = \begin{Bmatrix} e'_1 \\ \vdots \\ e'_m \end{Bmatrix}, \quad E^d = \begin{Bmatrix} e''_1 \\ \vdots \\ e''_m \end{Bmatrix} \quad (12)$$

where, DI denotes the defined damaged index, e'_i ($i=1,2,\dots,m$) is the mean value of the i^{th} line of the Euclidean norm matrix, E_{norm} in Eq. (9), of the intact structure. Similarly, e''_i ($i=1,2,\dots,m$) is for the damaged structure. E^u and E^d denote the average Euclidean norm of the intact and damaged structure respectively.

More effort is made as described below to improve the robustness of the damage index defined in Eq. (11). E^u in Eq. (12) is transformed to R^u in Eq. (13) for the intact structure. Similarly, E^d in Eq. (12) is transformed to R^d for the damaged structure. The damage index using R^u and R^d is defined in Eq. (14).

$$R^u = \begin{bmatrix} \frac{e'_1}{e'_1} & \dots & \frac{e'_1}{e'_j} & \dots & \frac{e'_1}{e'_m} \\ \frac{e'_1}{e'_1} & \dots & \frac{e'_j}{e'_j} & \dots & \frac{e'_m}{e'_m} \\ \vdots & \ddots & \vdots & \ddots & \vdots \\ \frac{e'_1}{e'_1} & \dots & \frac{e'_i}{e'_i} & \dots & \frac{e'_i}{e'_i} \\ \frac{e'_1}{e'_1} & \dots & \frac{e'_j}{e'_j} & \dots & \frac{e'_m}{e'_m} \\ \vdots & \ddots & \vdots & \ddots & \vdots \\ \frac{e'_m}{e'_1} & \dots & \frac{e'_m}{e'_j} & \dots & \frac{e'_m}{e'_m} \\ \frac{e'_1}{e'_1} & \dots & \frac{e'_j}{e'_j} & \dots & \frac{e'_m}{e'_m} \end{bmatrix} \quad (i=1,2,\dots,m; j=1,2,\dots,m) \quad (13)$$

$$DI'_{ij} = \left(\frac{R^d_{ij} - R^u_{ij}}{R^u_{ij}} \right)^2 \quad (14)$$

where DI'_{ij} is the i^{th} row and j^{th} element of the damaged index matrix, R^d_{ij} and R^u_{ij} are the i^{th} row and j^{th} column element in the matrices R^u and R^d respectively. If the damage occurs on the i^{th} element, the i^{th} row and the i^{th} column of the damage index matrix will change.

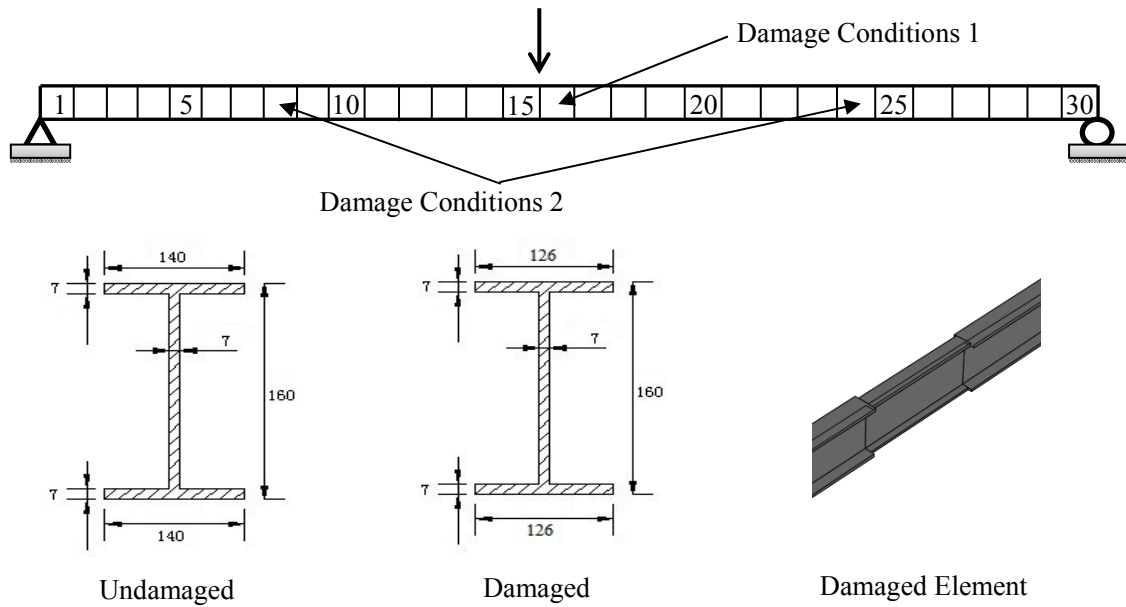


Fig. 2 The intact and damaged beam conditions

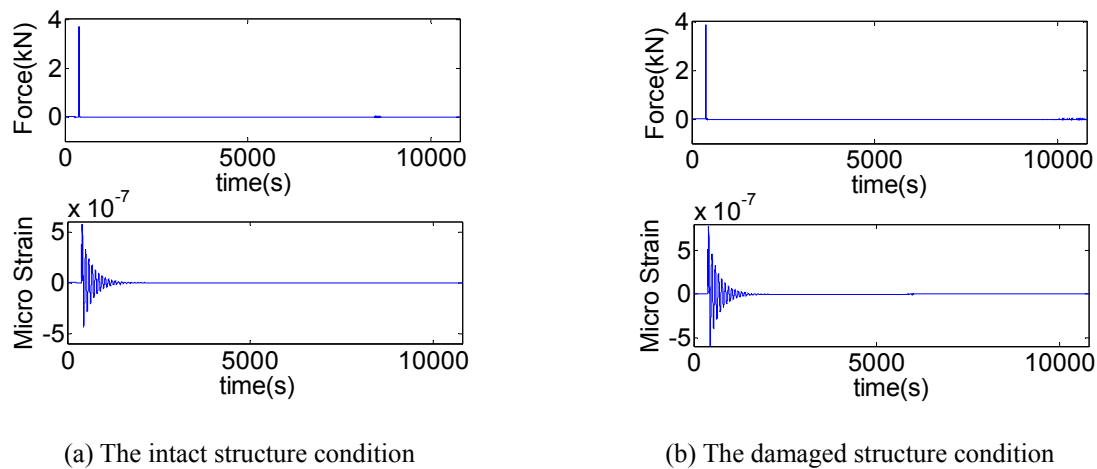


Fig. 3 Two sets of impacts and long-gauge fiber strain

4. Example investigation: a simple supported beam

For readers' easy understanding, the proposed method is first illustrated by taking a simple supported beam (Fig. 2) as an example. The beam has a length of 6 m, which is equally divided into 30 elements. Other than the intact structure, two damage cases are studied: (i) 10% stiffness loss of the 16th beam element, and (ii) 10% stiffness loss of the 8th and 24th beam elements. The stiffness loss is simulated by reducing the flange width of the beam element. Assuming long-gauge

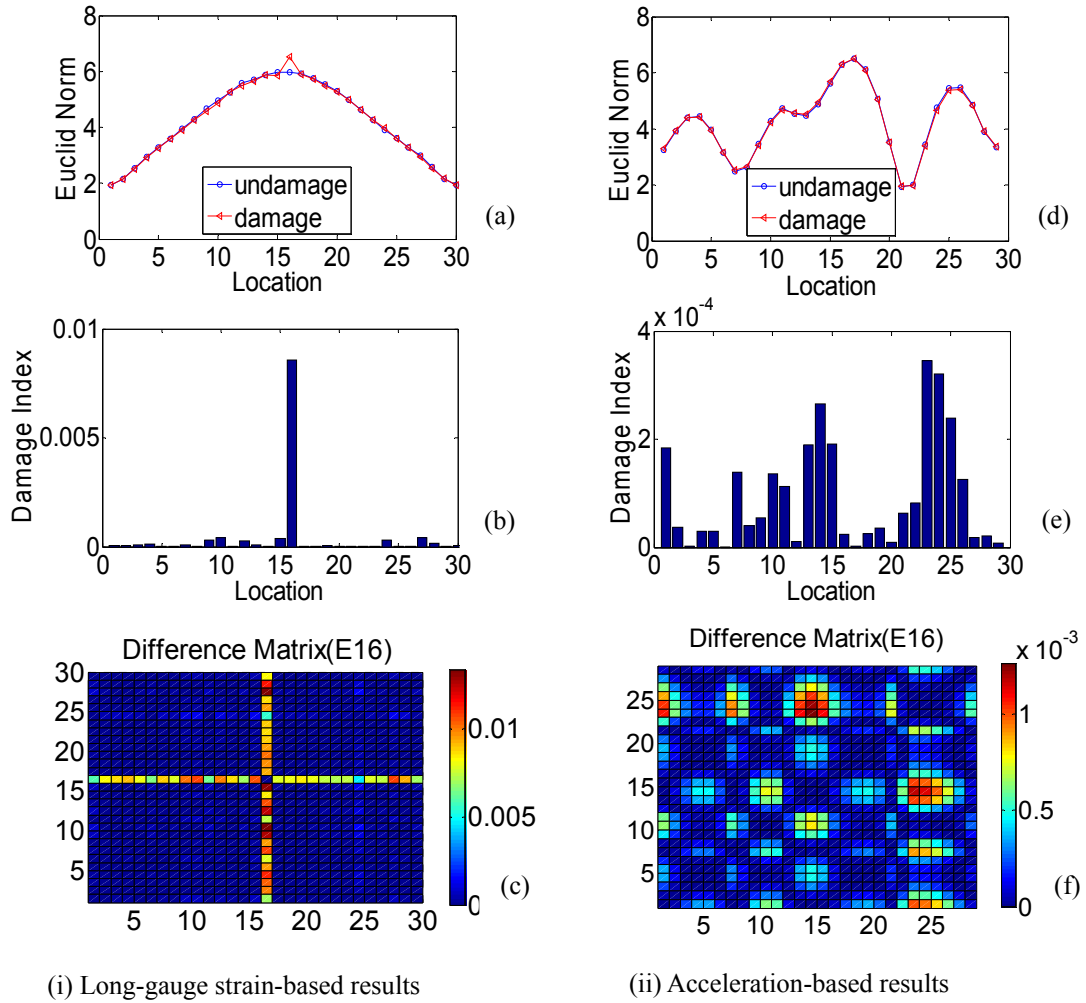


Fig. 4 Damage detection results of the damage condition (i)

FBG sensors with the gauge length of 0.2 m are mounted at the bottom of all beam elements for strain measurements. Impact tests of the intact and damaged structures are simulated in the SAP2000 software respectively. The impacting force measured during the hammer impact testing in the laboratory is applied to the beam central node for dynamic analyses. Fig. 3 shows the typical impacting force and long-gauge strain response of the intact structure and the damaged structure respectively. 10% white noise is added into the simulated data to represent the observation noise, in which 10% means that the standard deviation of the noise is 10% of that of the simulated macro strain.

The long-gauge dynamic strain responses during the impact testing are processed by using the proposed method. Principle components are first calculated through Eq. (8), then their Euclidean norms are calculated through Eq. (9). Finally the defined indexes in Eq. (11) and Eq. (14) are calculated respectively. Fig. 4(a)-(c) illustrates the damage detection results for the damage

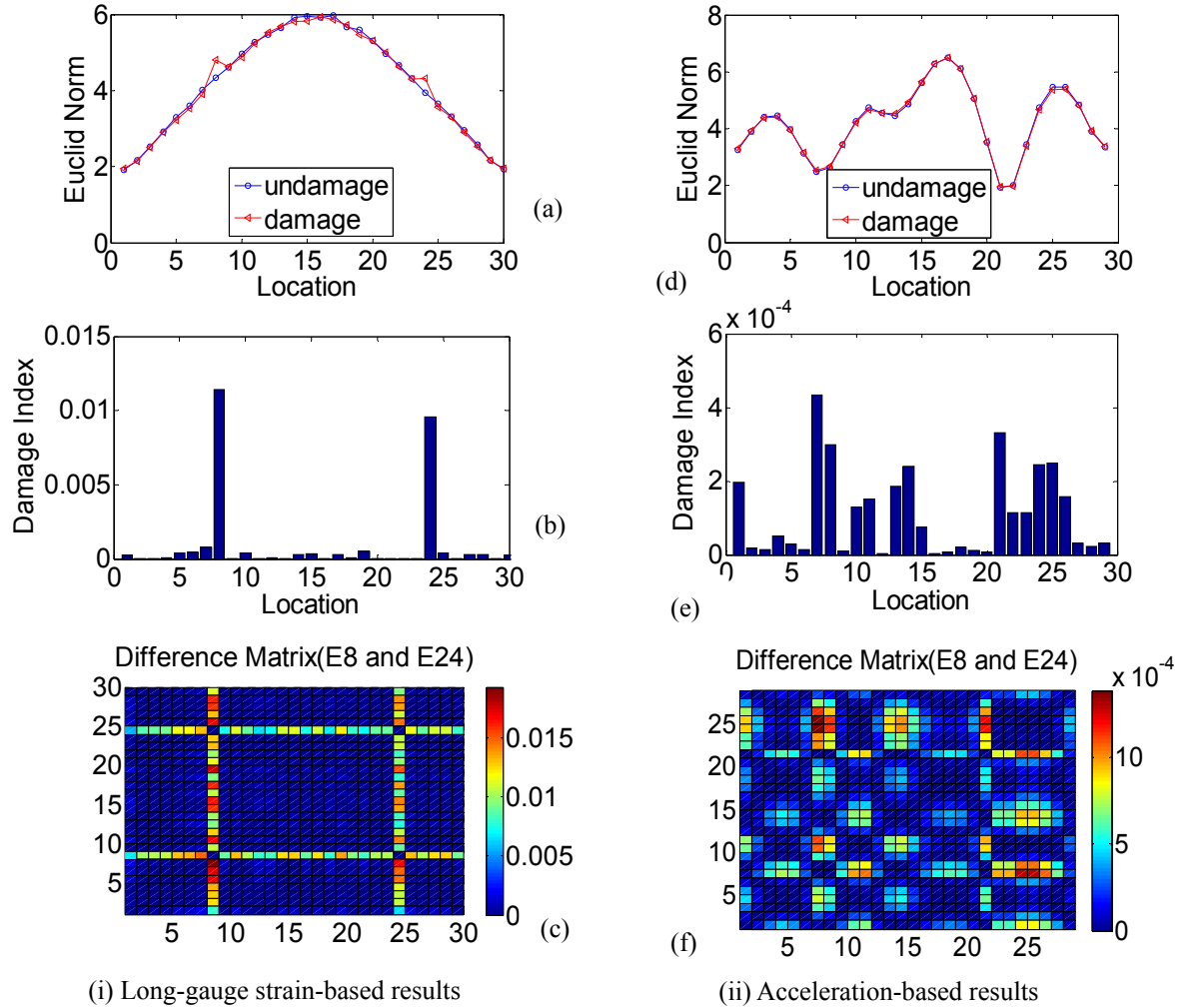


Fig. 5 Damage detection results of the damage condition (ii)

condition (i), i.e., the single damage condition. Fig. 4(a) shows the calculated Euclidean norms of the intact and damaged structures. Fig. 4(b) illustrates the damage index calculated from Eq. (11), in which the high index value corresponding the 16th elements indicates that the proposed method successfully identifies damage localization. Fig. 4(c) shows the damage index calculated from Eq. (14). The high values of the 16th row and column of the damage index matrix also reveal that the damage occurs on the 16th element. For comparison, the similar procedure to process the acceleration data during the impact test is also made and the results are shown in Fig. 4(d)-(f). It is seen that the proposed method using the long-gauge strain measurements is effective for damage detection, while the similar procedure using acceleration measurements fails to identify the damage location.

Similarly, Fig. 5(a)-(c) show the damage detection results for the damage condition (ii). It is seen that two damage indexes calculation from Eq. (11) and Eq. (14) successfully identify damage

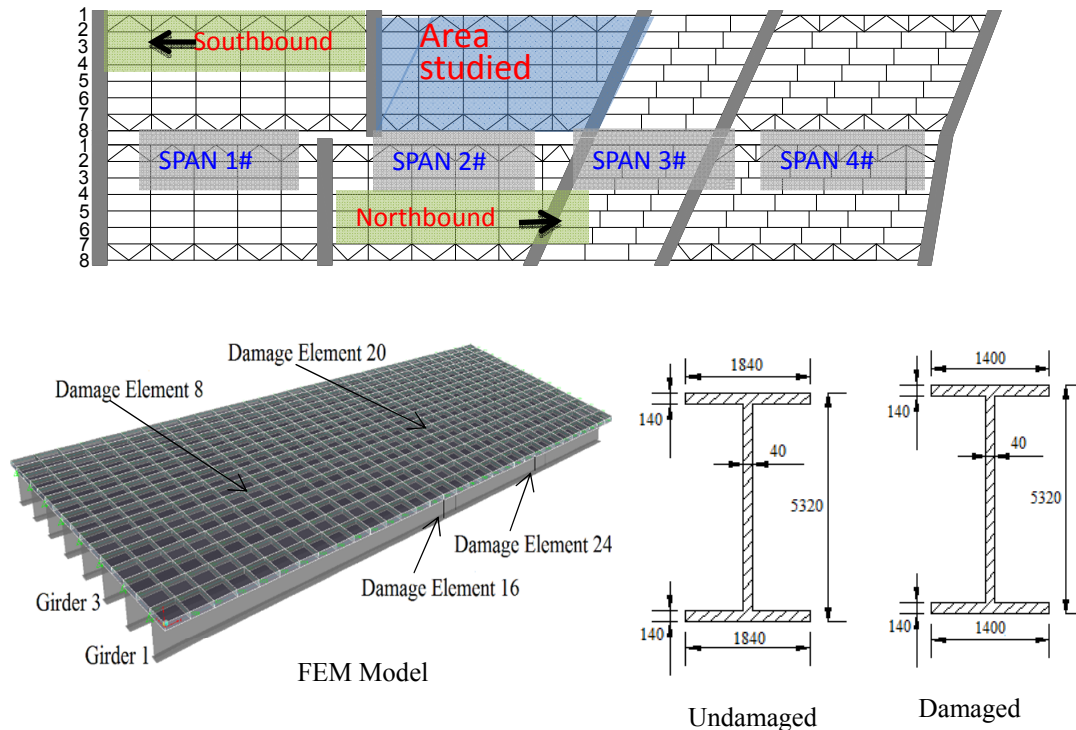


Fig. 6 The steel stringer bridge model

locations at the 8th and 24th elements, while the results from accelerations as shown in Fig. 5(d)-(f) fails to do that. The above comparison illustrates the advantage of the proposed method by using the long-gauge strain sensing technology.

5. Example investigation: a steel stringer bridge

The example of a steel stringer bridge is further studied to verify the proposed method. The investigated bridge is a multi-girder steel stringer bridge as shown in Fig. 6. It has four spans with a standard steel stringer design of girders, and each span is simply supported with pin and rocker bearings. Because it is unable to make damages on the real bridge, damage simulation is made in Sap2000 software. The finite element model is a combination of beam elements and shell elements used to simulate the steel girders and concrete deck as shown in Fig. 6. The concrete is modeled as a plate with a constant thickness of 24 cm. The concrete material is defined with an elastic modulus of 2×10^5 MPa and a density of 2400. Eight girders are modeled with beam elements whose dimensions are the same as those of the tested bridges. The model has the same skew as the tested bridge. The FE model is simply-supported at two ends. It totally includes 516 nodes, 256 frame elements, and 512 shell elements. Other than the intact structure, a damaged structure is also simulated by making 1.5% stiffness loss on the elements 16 and 24 of girder 1 and elements 8 and 20 of girder 3. Dynamic analyses of the intact and damaged structures are performed to simulate impact test data. For instance, girder 3 as shown in Fig. 6 includes 33 beam elements with the

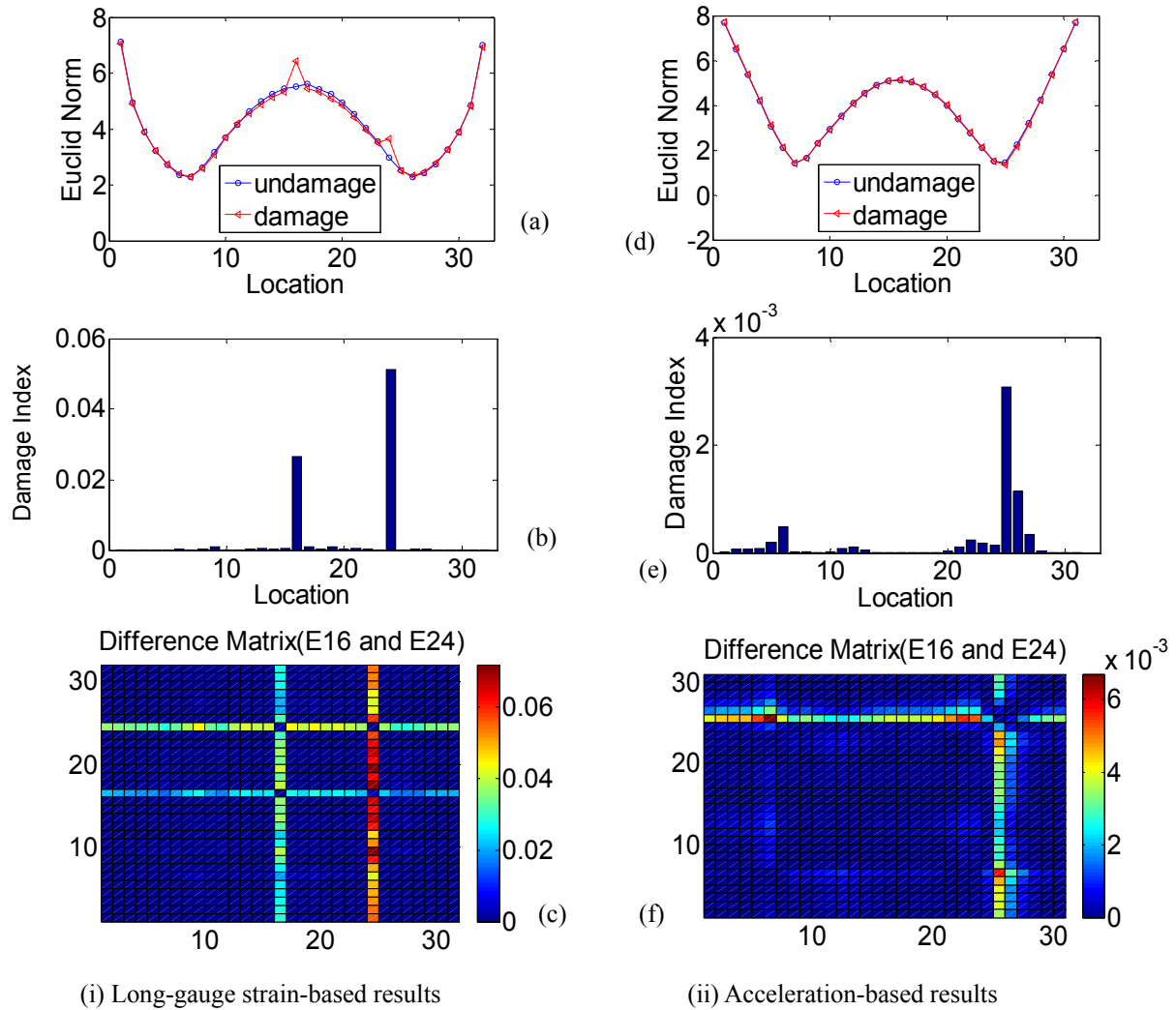


Fig. 7 Damage detection results of the girder 1

number 1 to 33 from left to right. The analyzed strain data for those 33 beam elements simulate the measurements from long-gauge strain sensors mounted on those elements. 10% white noise is added into the simulated data to represent the observation noise.

Damage detection results of the Girder 1 using the proposed method by processing the long-gauge strain responses are shown in Fig. 7(a)-(c). It is seen that the damages on the elements 16 and 24 are successfully identified, while the results by processing the acceleration responses as shown in Fig. 7(d)-(f) fail to identify damage locations. The damage detection results of the Girder 2 illustrate the similar findings.

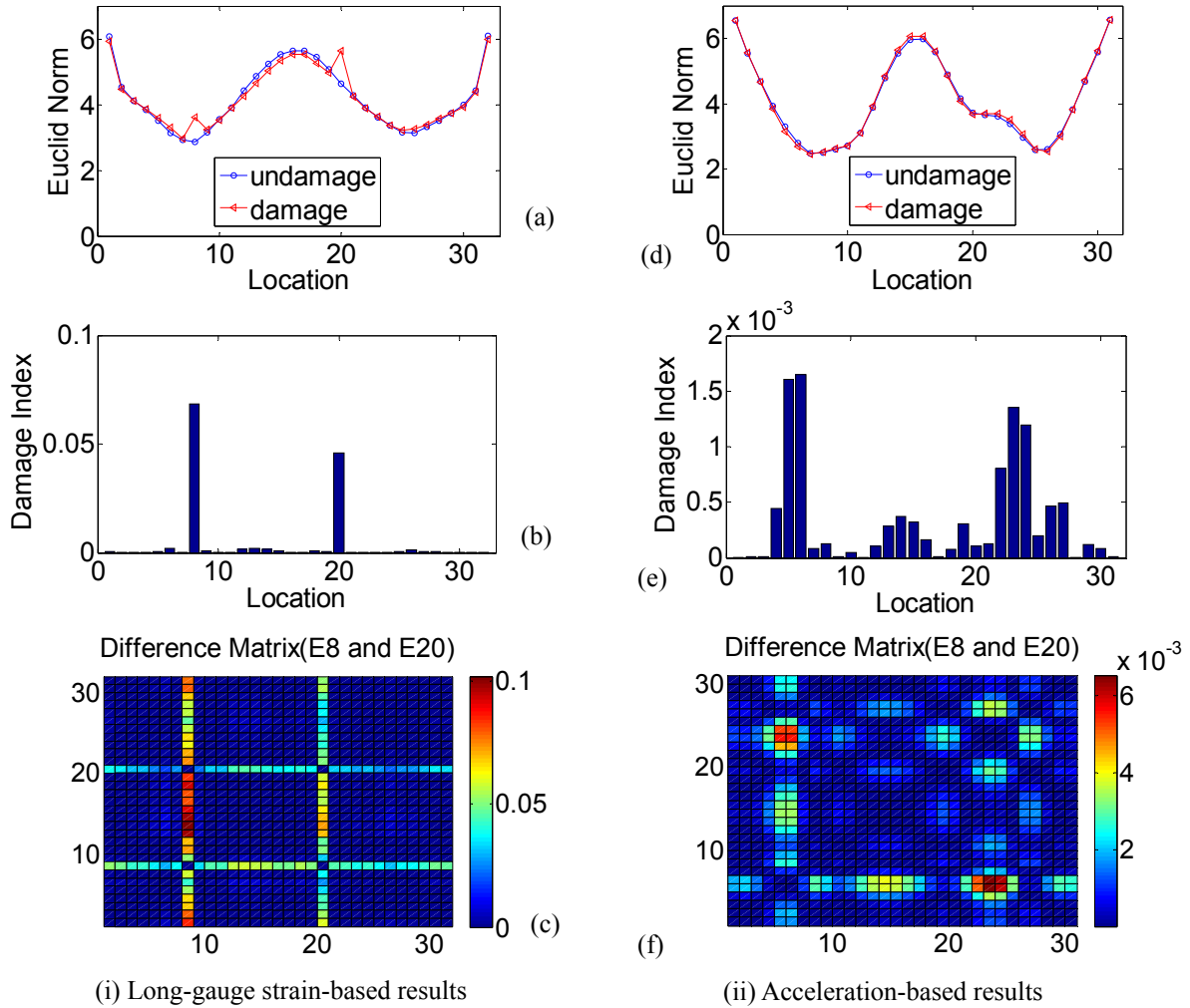


Fig. 8 Damage detection results of the girder 2

6. Conclusions

A damage detection method integrating the long-gauge fiber optic sensor and the principle component analysis (PCA) technologies has been proposed. In the proposed method, two new damage indexes have been defined by using the Euclidean norm of the principal components of long-gauge dynamic strains.

Examples have been investigated to illustrate how to use the proposed method for structural damage detection. By comparing the results from the long-gauge strains and accelerations, it is found that the proposed method using the long-gauge strains are effective for damage detection while the similar procedure using the acceleration responses are ineffective.

It should be noted that the proposed method is effective on the condition that the input forces

on the intact and damaged structures are close, for instance, the impact testing case studied in this article, in which the impacting forces can be controlled to be close by using the same equipment of impacting. In the condition of input forces are different, new methods should be further explored.

Acknowledgements

This work was sponsored by the National Science Foundation of China (51108076) and the National Thousand Talents program for young scholars.

References

- Adewuyi, A.P. and Wu, Z.S. (2011), "Modal macro-strain flexibility methods for damage localization in flexural structures using long-gage FBG sensors Struct", *Control Hlth. Monit.*, **18**, 341-60.
- Aditi, M., Ambar, De., Damodar, M. and Dipak Kumar, M. (2013), "Damage assessment of beams from changes in natural frequencies using ant colony optimization", *Struct. Eng. Mech.*, **45**(3), 391-410.
- Alvandi, A. and Cremona, C. (2006), "Assessment of vibration-based damage identification techniques", *J. Sound Vib.*, **292**, 179-202.
- An, Y. and Ou, J. (2012), "Experimental and numerical studies on damage localization of simply supported beams based on curvature difference probability method of waveform fractal dimension", *J. Intell. Mater. Syst. Struct.*, **23**, 415-26.
- Bagchi, A., Humar, J., Xu, P. and Noman, A.S. (2010), "Model-based damage identification in a continuous bridge using vibration data", *J. Perform. Constr. Facil.*, **24**(2), 148-158.
- Catbas, F.N., Brown, D.L. and Aktan, A.E. (2006), "Use of modal flexibility for damage detection and condition assessment: Case study and demonstrations on Large Structures", *J. Struct. Eng.*, **132**(11), 1699-1712.
- Conte, J.P., He, X.F., Moaveni, B., Masri, S.F., Caffery, J. P., Wahbeh, M., Tasbihgoo, F., Whang, D.H. and Elgamal, A. (2008), "Dynamic testing of Alfred Zampa Memorial Bridge", *J. Struc. Eng.*, **134**(6), 1006-1015.
- Ratcliffe, C.P. (1997), "Damage detection using a modified Laplacian operator on mode shape data", *J. Sound Vib.*, **204**(3), 505-517.
- Doebeling, S.W., Farrar, C.R. and Prime, M.B. (1998), "A Summary of Vibration-based damage identification methods", *Shock Vib. Dig.*, **30**, 91-105.
- Guan, H. and Karbhari, V.M. (2008), "Improved damage detection method based on element modal strain damage index using sparse measurement", *J. Sound Vib.*, **309**, 465-94.
- He, X.F., Moaveni, B., Conte, J.P., Elgamal, A. and Masri, S.F. (2009), "System identification of Alfred Zampa Memorial Bridge using dynamic field test data", *J. Struct. Eng.*, **135**(1), 54-66.
- Santos, J.P., Orcesi, A.D., Crémona, C. and Silveira, P. (2015), "Baseline-free real-time assessment of structural changes", *Struct. Infrastr. Eng., Main. Manag. Life-Cycl. Des. Perform.*, **11**(2), 145-161.
- Kazemi, S., Fooladi, A. and Rahai, A.R. (2010), "Implementation of the modal flexibility variation to fault identification in thin plates", *Acta Astronaut.*, **66**, 414-26.
- Lei, Y., Jiang, Y.Q. and Xu, Z.Q. (2012), "Structural damage detection with limited input and output measurement signals", *Mech. Syst. Signal Pr.*, **28**, 229-243.
- Lei, Y., Wu Y. and Li, T. (2012), "Identification of nonlinear structural parameters under limited input and output measurements", *Int. J. Nonlin. Mech.*, **47**, 1141-1146.
- Li, S.Z. and Wu, Z.S. (2007), "Development of distributed long-gage fiber optic sensing system for structural health monitoring", *Struc. Health Monit.*, **6**(2), 133-143.
- Mehmet, E.A. and Durmus, A. (2014), "Modal parameter identification of in-filled RC frames with low

- strength concrete using ambient vibration”, *Struct. Eng. Mech.*, **50**(2), 137-149.
- Yoon, M.K., Heider, D., Gillespie Jr., J.W., Ratcliffe, C.P. and Crane, R.M. (2005), “Local damage detection using the two-dimensional gapped smoothing method”, *J. Sound Vib.*, **279**, 119-139.
- Montalvao, D., Mafia, N.M. M. and Ribeiro, A. M. R. (2006), “A review of vibration-based structural health monitoring with special emphasis on composite materials”, *Shock Vib. Dig.*, **38**, 295-234.
- Rezaiee-Pajand, M. and Kazemiyan, M.S. (2014), “Damage identification of 2D and 3D trusses by using complete and incomplete noisy measurements”, *Struct. Eng. Mech.*, **52**, 149-172.
- Ni, Y.Q., Zhou, X.T. and Ko, J.M. (2006), “Experimental investigation of seismic damage identification using PCA-compressed frequency response functions and neural networks”, *J. Sound Vib.*, **290**, 242-263.
- Yazdanpanah, O., Seyedpoor, S.M. and Akbarzadeh Bengar, H. (2015), “A new damage detection indicator for beams based on mode shape data”, and **53**(4), 725-744.
- Rucevskis, S. and Wesolowski, M. (2010), “Identification of damage in a beam structure by using modal shape curvature squares”, *Shock Vib.*, **17**, 601-10.
- Zhang, J., Prader, J., Grimmelsman, K.A., Moon, F., Aktan, A.E. and Shama, A. (2013), “Experimental vibration analysis for structural identification of a Long-Span suspension bridge”, *J. Eng. Mech.*, **139**(6), 748-759.
- Zhang, J., Hong, W., Tang, Y.S., Yang, C.Q., Wu, Q. and Wu, Z.S. (2014), “Structural health monitoring of a steel stringer bridge with area sensing”, *Struct. Eng. Mech.*, **10**(8), 1049-1058.
- Zou, Y., Tong, L. and Steven, G.P. (2000), “Vibration based model-dependent damage (delamination) identification and health monitoring for composite structures-a review”, *J. Sound Vib.*, **230**, 357-378.